Hindawi
Shock and Vibration
Volume 2021, Article ID 6165198, 12 pages
https://doi.org/10.1155/2021/6165198

Research Article

Experimental Study on Percolation Rate Characteristics of Gas-Filled Coal Bodies Based on True Triaxial Condition

Xiao Fukun[1,2], **Shan Lei**[2], **Zhang Xufei**[2], and **Xie Kai**[2]

[1]*Heilongjiang Ground Pressure & Gas Control in Deep Mining Key Laboratory, Heilongjiang University of Science and Technology, Harbin, Heilongjiang 150022, China*
[2]*College of Mining Engineering of Hust, Heilongjiang University of Science and Technology, Harbin, Heilongjiang 150022, China*

Correspondence should be addressed to Shan Lei; 735768833@qq.com

Received 9 October 2021; Accepted 8 November 2021; Published 22 November 2021

Academic Editor: Xing-Dong Zhao

To research the percolation rate of gas-filled coal based on true triaxial condition, this paper uses the three-phase coupling true triaxial servo test device to carry out the seepage test of coal, and the percolation rate of coal under different conditions of three factors such as gas pressure was measured by Darcy's law, and the variation of percolation rate of coal was studied based on the comprehensive consideration of thermal elastic swelling deformation, expansion deformation of adsorbed gas, and compression deformation of interstitial pressure. The results are as follows: (1) When the main stress and temperature maintain unchanged, the percolation rate presents the trend which first decreases and then becomes gentle with the gas pressure; when the gas pressure and main stress maintain unchanged, the percolation rate increases with the decrease of temperature; when the pressure and temperature maintain unchanged, the changes of percolation rate present a shape of "V" with the main stress. (2) The strain curve of gas-filled coal decreases at first and then increases; that is, the percolation rate decreases gradually when the strain increases at the compression phase and elastic phase, while the percolation rate increases with the increase of strain at the yield phase and failure phase. (3) In the process of increasing volume stress, the percolation rate decreases gradually in the pore compaction stage, the percolation rate increases gradually from crack propagation to peak failure stage, and then, the percolation rate increases significantly after the peak damage. According to the test results, the percolation rate and volume strain show an inverse proportion.

1. Introduction

Gas anomalies easily lead to dynamic disasters in mines, such as gas outburst accidents. Gas dynamic disasters are one of the main disasters in mines in China. At the same time, gas is also a clean and efficient energy source; therefore, improving the level of gas extraction is important to alleviate the energy shortage and reduce the occurrence of gas disasters. The percolation rate characteristics of coal bodies are closely related to gas. It may change the mechanical properties of the coal as it absorbs gas, such as the expansion stress from adsorption expansion deformation, coal rock strength reduction, etc. It will also change the temperature field, pressure field, and strain field of the coal body. Numerous scholars have conducted studies on the percolation rate characteristics of gas-filled coal bodies [1–25]. Xiao et al. [1, 2] studied the gas gushing pattern along the bottom slab and explored the influence of mining on the bottom slab and gas extraction at the working face, thereby providing a basis for the study of the percolation rate change pattern at the site. Yu et al. [3, 4] carried out experimental study on coal seepage to explore the effects of temperature, axidirection pressure, and surrounding pressure on the percolation rate of coal type. Jiang et al. [5, 6] investigated the influence of temperature on the percolation rate of raw coal under the condition of triaxial stress and gas pressure through true triaxial test; they found that the temperature and percolation rate were inversely related. Yin et al. [7] conducted a full stress-strain gas percolation experiment on the gas-filled coal bodies and investigated the relationship among axial strain, axial stress, and percolation rate. Wang et al. [8, 9] carried out a study on the connection between the absolute counts of the difference between axidirection pressure and circumferential pressures and the percolation rate. Cheng [10] studied the evolution law of coal seepage properties in solid-gas coupling tests.

Most of the above research results are based on scientific research under monopodium or false three-axis condition, without the comprehensive consideration of the influence of coupling temperature, in situ stress, and gas pressure. The actual coal bodies in coal seams are under a three-dimensional stress, and the mechanical activation behavior of coal, gas pressure, in situ stress, and temperature has important joint effects on the percolation rate characteristics of coal bodies during the coal mining process. In view of the shortcomings in the above study, to study the seepage of gas in a more realistic way, this paper explores the change law of percolation rate of gas-filled coal bodies by conducting a seepage test study of raw coal under true triaxial conditions with the self-developed thermal-solid-gas coupling test device and analyzes the full stress-strain and percolation rate of gas-filled coal bodies. In addition, the connection between total stress-strain and percolation rate of gas-filled coal bodies and the influence of volumetric stress and volumetric strain on percolation rate were analyzed, which provided a theoretical basis for the prophylaxis and treatment of gas power disasters and the improvement of gas drainage effect.

2. Experimental Studies

2.1. Specimen Preparation. The coal block for the test was taken from the sixth mining area of 32 coal seam of Donghai Coal Mine in Jixi City, which is soft and fragile, containing more laminae and fissures. The original coal specimen was cut out by a cutting machine in the direction of fissure and joint development, as shown in Figure 1. And the specimen was machined to the size of 50 mm × 50 mm × 100 mm with smooth surface all around with a grinder; after that, the coal sample was dried in a drying oven. The fundamental mechanics parameters of the coal body were determined by the experiment, as shown in Table 1.

2.2. Test Setup. The core equipment of this paper is the solid-thermal-gas three-phase coupling true triaxial servo experimental device, which can be used to realize true triaxial test. This device is the joint research result of the key laboratory and the experimental equipment manufacturing company. Its biggest advantage is to achieve true triaxial test, true triaxial, and false triaxial although there is only one word difference, but the actual effect is really a world of difference. At the same time, it can also set different parameters of gas pressure field, temperature field, and stress field, so as to explore the seepage characteristics of coal and rock mass under different physical fields. The device consists of six big systems, which are provided by the servo press test required load loading system, measuring stress-strain continuous variation in the process of experimental measurement system; gas such as gas supply, gas pressure constant supply is needed to generate test system; with the simulation of the temperature field control system, test seepage occurs in the process of traffic monitoring system, computer terminal data recording, and manipulation system. The thermal-solid-gas coupling experimental setup is shown in Figure 2 [11].

2.3. Testing Program. To study the relationship among gas pressure, temperature, stress, and percolation rate, as well as the relationship between total stress-strain and percolation rate of gas-filled coal bodies, and the effect of volumetric stress and volumetric strain on the percolation rate of coal bodies, the following test procedures were developed in this paper.

(1) Load the square coal sample prepared by the test into the fixture reasonably, with assembly of the loading indenter, gas supply line, and sensor. Check the working state of the screw, and inspect all connection locations to ensure airtightness of pipeline in experiment. Prepare vacuum for the specimen continuously for 1 h with the vacuum pump; then, open the valve and feed in gas continuously for 1 h, so that the specimen and pipeline are under the saturated gas.

(2) Keep the gas pressure at 0.3 MPa and three main stresses at $\sigma_1 = 3$ MPa, $\sigma_2 = 2$ MPa, and $\sigma_3 = 4$ MPa, respectively. In the meantime, the test temperature is heated to 30°C, 40°C, 50°C, 60°C, and 70°C, respectively, through the thermostat box heater in turn, and the temperature is kept for 1 hour, respectively, before measuring the coal percolation rate.

(3) Keep the temperature at 30°C and the three main stresses are unchanged, i.e., $\sigma_1 = 3$ MPa, $\sigma_2 = 2$ MPa, and $\sigma_3 = 4$ MPa. Apply gas pressure to the test piece through the gas pressure regulating system, so that the gas pressure increases to 0.3 MPa, 0.6 MPa, 0.9 MPa, 1.2 MPa, and 1.5 MPa in turn, respectively, and then stabilize the air pressure for 30 min before measuring the coal body percolation rate.

(4) Keep the gas pressure at 0.3 MPa and the temperature at 30°C; in the meantime, keep the two main stresses unchanged, i.e., $\sigma_1 = 3$ MPa and $\sigma_3 = 4$ MPa. Water was injected into the experimental device through the servo pump, and the coal percolation rate was measured when σ_2 was increased from 2 MPa to 10 MPa in the step length of 2 MPa by means of water pressure and kept for 0.9 h.

(5) Due to the anisotropy and complex internal structure of the raw coal, to prevent the occurrence of test errors and exceptions, the coal body needs to be tested for several times under different conditions. That is, maintain the gas pressure at 0.6 MPa and 0.9 MPa and the principal stress at 4 MPa and 6 MPa, respectively, and repeat Step (2); maintain the temperature at 50°C and 70°C and the principal stresses at $\sigma_2 = 4$ MPa and $\sigma_2 = 6$ MPa, respectively,

Figure 1: Specimens of raw coal.

Table 1: Fundamental mechanics parameter of coal samples.

Density (g/cm^3)	Modulus of elasticity (MPa)	Poisson's ratio	Volume compression factor	Water content (%)
1.45	2700	0.26	7.7×10^{-4}	1.2

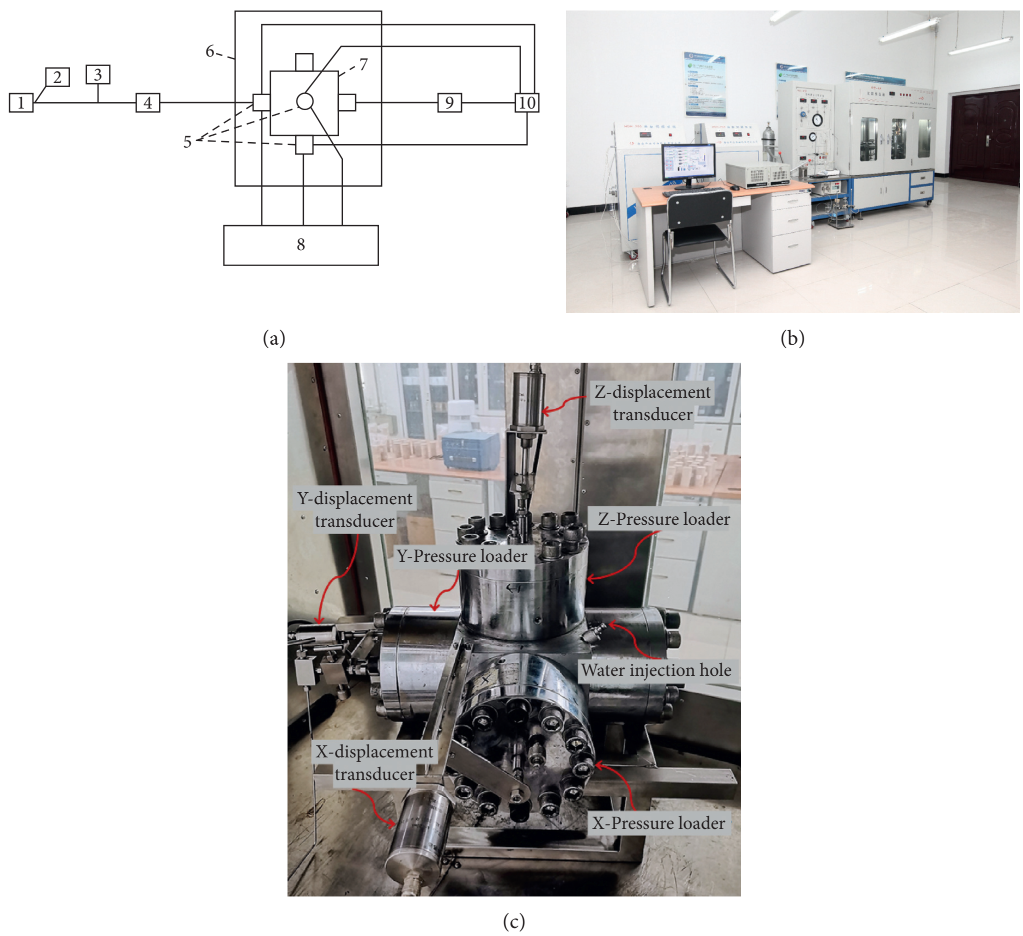

Figure 2: Thermos-solid-gas coupling equipment. (a) Frame diagram of true triaxial experimental equipment. 1, gas supply cylinder; 2, pressure meter; 3, control valve; 4, pressure regulating system; 5, stress-strain and temperature sensor; 6, constant temperature test chamber; 7, true triaxial fixture; 8, servo pump; 9, flow surveillance system; 10, data acquisition and operating system; (b) true triaxial equipment drawing. (c) True triaxial clamping device.

and repeat Step (3); maintain the gas pressure at 0.6 MPa and 0.9 MPa and the temperature at 50°C and 70°C, respectively, and repeat Step (4). The damage of coal sample is shown in Figure 3.

2.4. Penetration Rate Calculation. In this test, Darcy's law is used to calculate the percolation rate of gas-filled coal bodies under different conditions. The formula for calculating the percolation rate of coal in this test is as follows:

Figure 3: Coal sample failure diagram.

$$K = \frac{2Qp_0\mu L}{A\left(p_1^2 - p_2^2\right)}, \tag{1}$$

where "K" refers to the percolation rate (m^2); "A" represents the cross-sectional area of the specimen (mm^2); and "P_1" represents the gas pressure at the entrance (MPa); "P_2" denotes the gas pressure at the exit (MPa); "Q" refers to the amount of gas seepage in standard coal samples (mL/s); "p_0" represents the barometric pressure for the measuring point, at the standard atmospheric pressure selected at 0.101325 MPa; "μ" denotes the viscosity factor of the gas (MPa·s); "L" refers to the length of the standard samples (mm), respectively.

3. Experiment Results Analysis

3.1. Penetration Rate Change Characteristics. The prepared specimens were tested according to the proposed test protocol, and the percolation rate was calculated according to equation (1) to obtain the percolation rate of the specimens under different temperatures, gas pressures, and stress. The results are shown in Figures 4–6.

It can be seen from Figure 4 that when the temperature and principal stress remain unchanged during the test, if the gas pressure is maintained in the range of 0.3–0.9 MPa, increasing the pressure value will lead to a rapid decline in the permeability of coal samples. However, when it exceeds the limit of this range, the downward trend of permeability gradually tends to be flat. The reason for this phenomenon is that, in the process of controlling the increase of gas pressure, it is necessary to further increase the gas flow, which will lead to the increase of gas flow into the internal of the coal sample. At first, the gas will penetrate into the original cracks and pores in the coal sample. Since the defects in the coal sample have a certain volume, it can accommodate some of the gas penetrated, but with continuous absorption, it reaches the initial saturation. At this time, due to the external triaxial stress constraint, the coal sample cannot expand outward and can only continue to develop in the internal, resulting in the phenomenon of internal expansion. Under the continuous action of this phenomenon, the internal defects of coal samples are gradually compacted by gas; in that case, the channels available originally for gas infiltration are occupied, making the gas infiltration from the coal body more difficult, thereby resulting in lower percolation rate. From another perspective, in the process of increasing the pressure and gas flow volume, the gas content attached to the inner wall of the coal sample will also increase, making the thickness of the inner wall of the coal sample increase, which easily induces the decrease of the gas adhesion in the inner wall of the coal sample, which leads to the decrease of the permeability of the coal sample, which is the famous Klinkenberg effect phenomenon. However, the internal space of the coal body is limited; when the coal body adsorbs gas to a certain extent, the internal space is occupied completely, and the internal expansion effect will not occur anymore; therefore, the changes of the percolation rate become slow.

As shown in Figure 5, if the gas pressure and the main stress are constant, the percolation rate tends to decrease when the temperature increases from 30°C to 70°C. Firstly, the increase of temperature will lead to the increase of gas viscosity coefficient, and the gas flow in the coal body becomes slower, which is not beneficial for the gas permeation in the coal. On the side, the temperature plays a decisive role in the characteristics of the coal. The increase of temperature will lead to the softening and frangibility of the coal body, and the plasticity will be increased; therefore, the internal fissures and pores of coal body will be compressed more easily under the same conditions, thus resulting in the decrease of the percolation rate. According to the "thermal expansion and contraction effect," when the temperature increases, the coal body will undergo internal thermal expansion and deformation, which will squeeze the original fissures and pores and make the coal body more compact. Consequently, the gas will not penetrate easily, thereby resulting in the decrease of percolation rate.

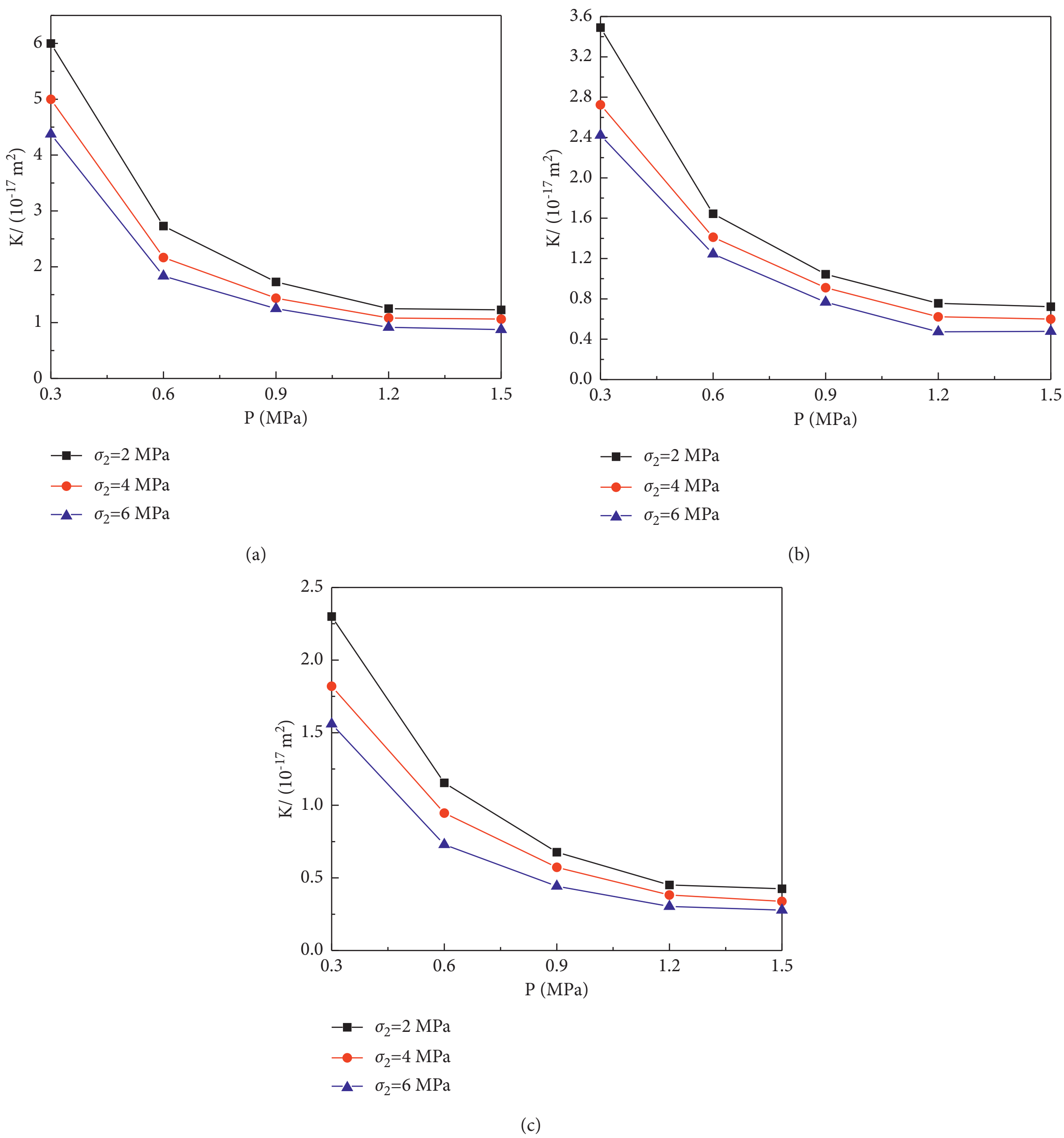

FIGURE 4: The effects of gas pressure on the percolation rate of coal sample at 30, 50, and 70°C and different stress. (a) T = 30°C. (b) T = 50°C. (c) T = 70°C.

As per Figure 6, in the process of increasing the principal stress, the change trend of seepage rate first decreases and then increases, and the overall change presents the shape of "V." When the main stress increases from 2 MPa to 8 MPa, the original defects of coal samples are gradually closed under pressure, and the cross-sectional area of fracture channel which can provide gas seepage is reduced, resulting in the decrease of seepage velocity. It can be seen that the percolation rate and principal stress are inversely proportional in a certain range. However, when it exceeds a certain range, due to the continuous increase of the principal stress, the internal defects of the coal sample are amplified, and the cracks and pores gradually extend and expand on the original basis until the shear failure of the coal sample. This will lead to shear expansion and expansion which makes the gas permeation happen more easily; consequently, the percolation rate increases.

3.2. Full Stress-Strain versus Percolation Rate Curve for Gas-Filled Coal Bodies. Figure 7 reveals the profile of stress and percolation rate versus strain under different gas pressures at T = 30°C, and the changes of the internal structure of the coal body have an important influence on the percolation rate. Initially, the gas is able to permeate the coal body due to the relatively large amount of pores and fissures in the raw coal,

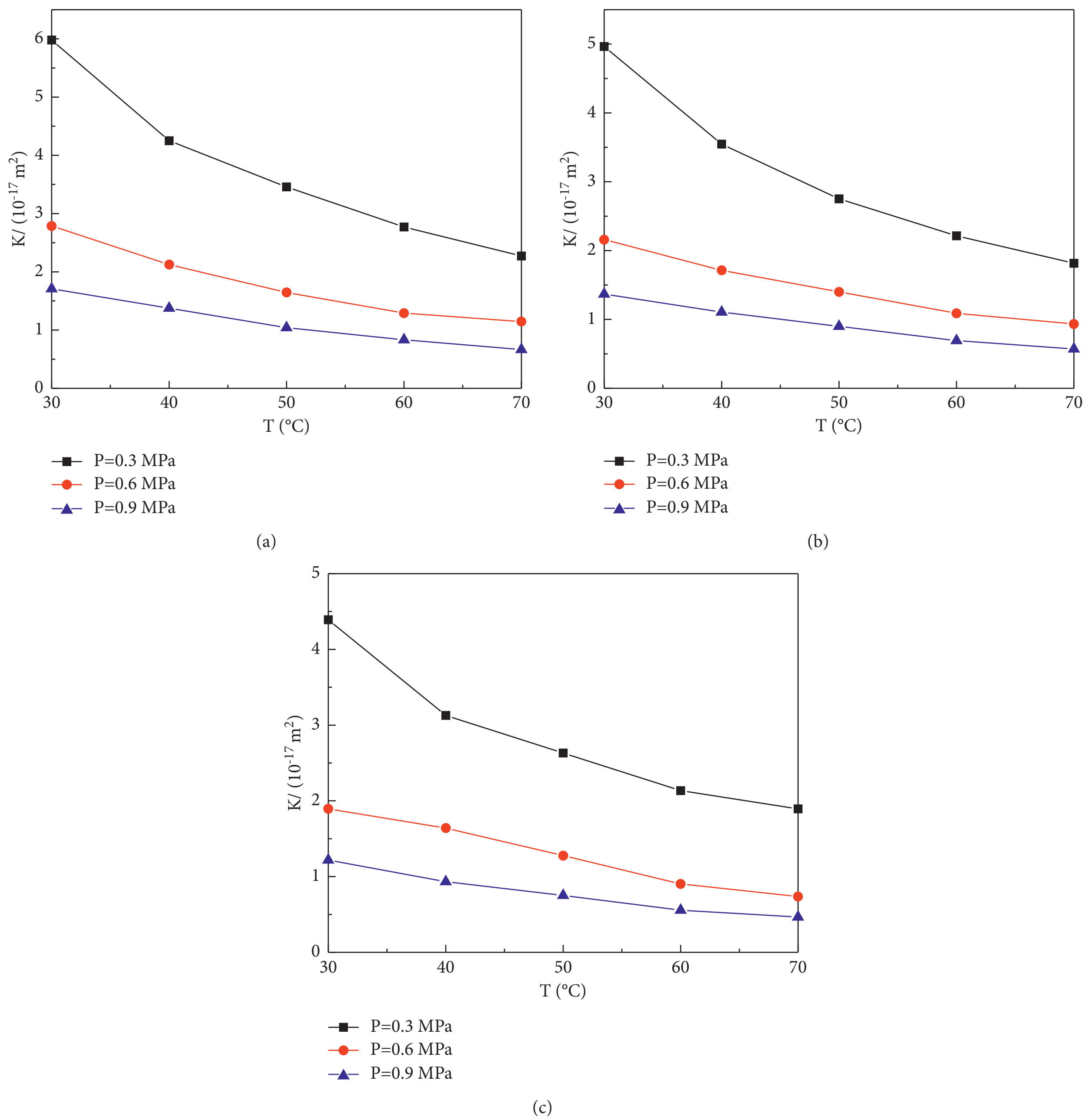

FIGURE 5: The effects of temperature on coal percolation rate with $\sigma_2 = 2$ MPa, 4 MPa, and 6 MPa at different gas pressures. (a) $\sigma_2 = 2$ MPa. (b) $\sigma_2 = 4$ MPa. (c) $\sigma_2 = 6$ MPa.

thus resulting in a relatively high initial percolation rate, while with the increase of the main stress, the original fracture pores are gradually compacted at the compacting and elastic stages, resulting in the decrease of seepage velocity. It can be seen that the percolation rate and principal stress are inversely proportional in a certain range. When the stress increases and enters the stage available to cause the yield deformation of coal body, the percolation rate and strain show a direct-proportion trend of change. This is because when the stress increases to the yield deformation stage, the fissures and pores inside the coal body tend to open and develop, and the greater the stress is, the more the fissures and pores will be produced inside, which further increases the seepage channel, and the trend for higher percolation rate appears. When the stress increases to a certain value, the original defects in coal samples began to expand and develop, and numerous tiny fissures gradually evolve to a few macroscopic large cracks, thus leading to the local damage of the coal body, i.e., local instability; in the meantime, the stress suddenly decreases. The macroscopic large cracks generated make the gas permeate more easily; thus, the percolation rate increases sharply. At the stage of residual stress, the fractures are fully developed, the opening and development of the fractures are mainly caused by the

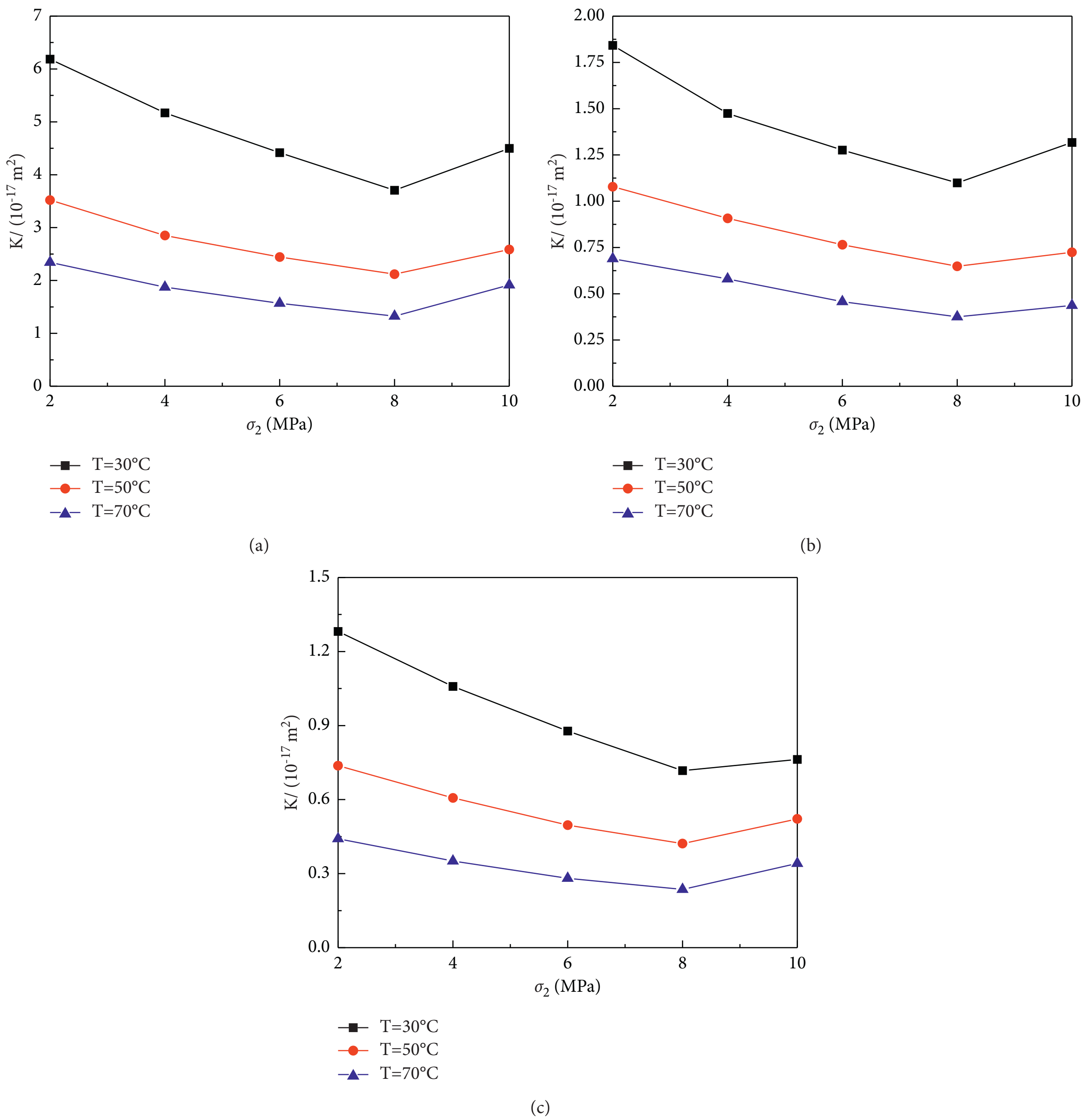

Figure 6: The effects of triaxial stress on the percolation rate of coal sample at $p = 0.3$ MPa, 0.6 MPa, and 0.9 MPa and different temperatures. (a) $p = 0.3$ MPa. (b) $p = 0.6$ MPa. (c) $p = 0.9$ MPa.

misalignment of the ruptured coal, and there are almost no large crack defects. The gas seepage channel is no longer expanded, so percolation rate can increase only slowly.

3.3. Characteristics of Volumetric Stress, Volumetric Strain, and Percolation Rate Variation. The fine changes, such as the expansion or compression of cracks and pores inside the coal body, have a certain decisive effect on percolation rate. And the volumetric stress indicates the sum of the three principal stresses applied to coal body; it can fully reveal the internal configuration variation of coal under stress. In this case, the research on the effect of confining pressure on permeability characteristics of gas-filled coal has practical meaning for coal mine safety production.

Figure 8 reveals the change profile of percolation rate versus volumetric stress of gas-filled coal body, from which it can be found that there are about 3 stages of development of volumetric stress versus percolation rate. At the beginning, the applied volumetric stress is relatively small, and when the volumetric stress increases, the fractures and pores inside the coal body do not expand accordingly; instead, they remain in

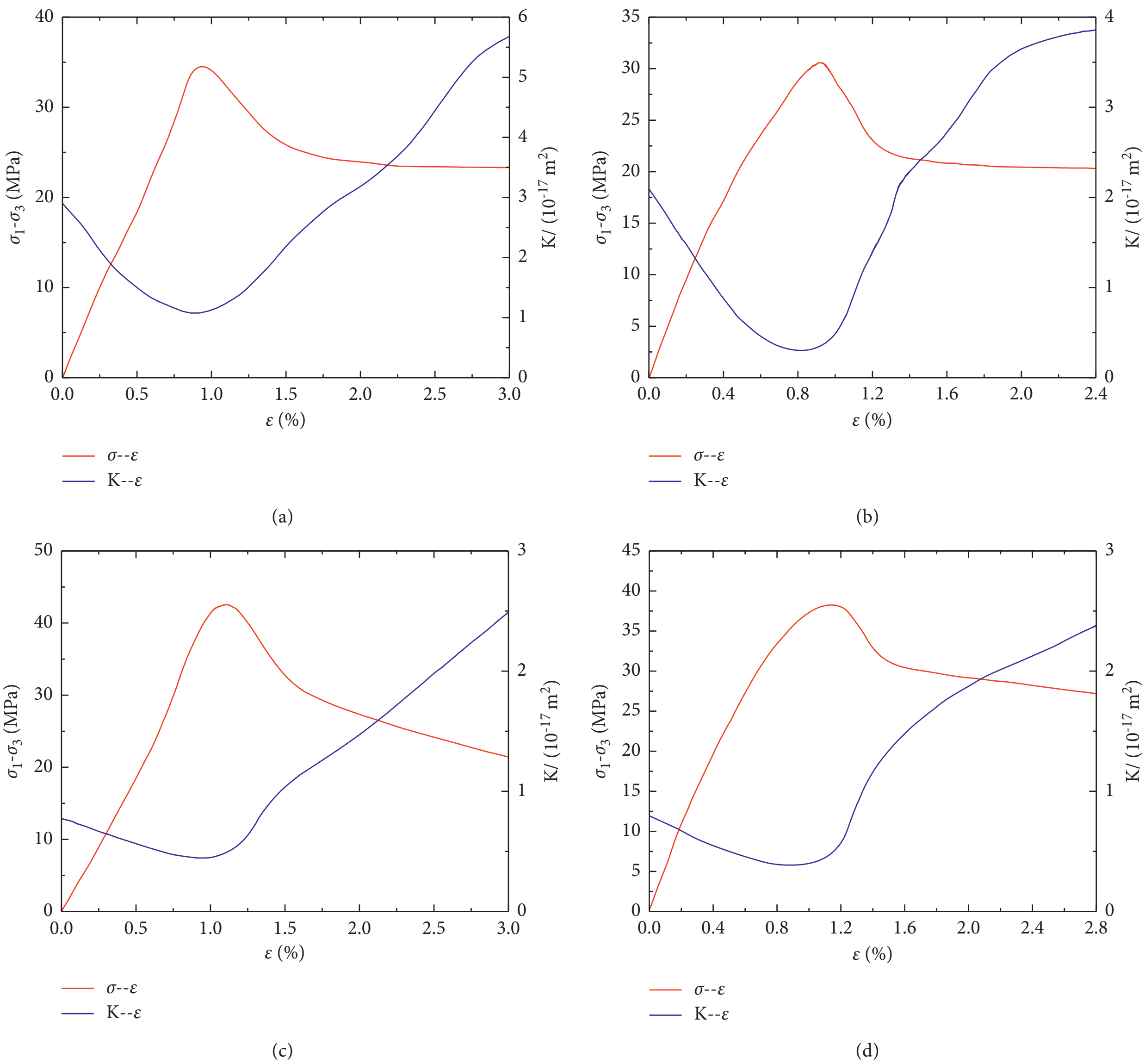

Figure 7: Profile of stress and permeability versus strain under different gas pressures at $T = 30^\circ$C. (a) $p = 0.3$ MPa. (b) $p = 0.6$ MPa. (c) $p = 0.9$ MPa. (d) $p = 1.2$ MPa.

the compressed state. With the original fissures and pores gradually compacted, it is more difficult for gas to penetrate; in the meantime, the gas seepage channels which are already narrow become narrower, and the gas seepage rate becomes slower, so the percolation rate decreases. When stress continued to increase the original defects in coal began to expand, and new cracks and pores gradually appear inside. The cracks lap and penetrate each other, so that the internal deformation damage of the coal body gradually increases, making it easier for gas to permeate, which results in the sudden increase of the percolation rate change. With more and more expansion of the internal cracks and pores, many tiny cracks start to penetrate and converge, resulting in the sudden destabilization of the coal body. Its original load-bearing structure is destroyed, resulting in the decrease of the load-bearing capacity and the decrease of volume stress. However, the percolation rate increases sharply, which may be due to the transformation of the original tiny cracks into macroscopic large cracks, thereby making it easier for gas to permeate, and the seepage channel which is blocked originally becomes smooth.

To reflect the regularity of percolation rate of gas-filled coal bodies and the evolution of coal body crack and pores more comprehensively, the relationship between volumetric strain and percolation rate was studied in this experiment. When the main stress on the coal body changes, not only does the axial strain change, but also the lateral strain changes. The volume strain can better reflect the effect of both changes, thus characterizing the internal fracture and pore evolution process of the coal body more macroscopically and obtaining the percolation rate change law, as shown in Figure 9.

The percolation rate and volume strain of the gas-filled coal body include two main characteristic stages, as shown in

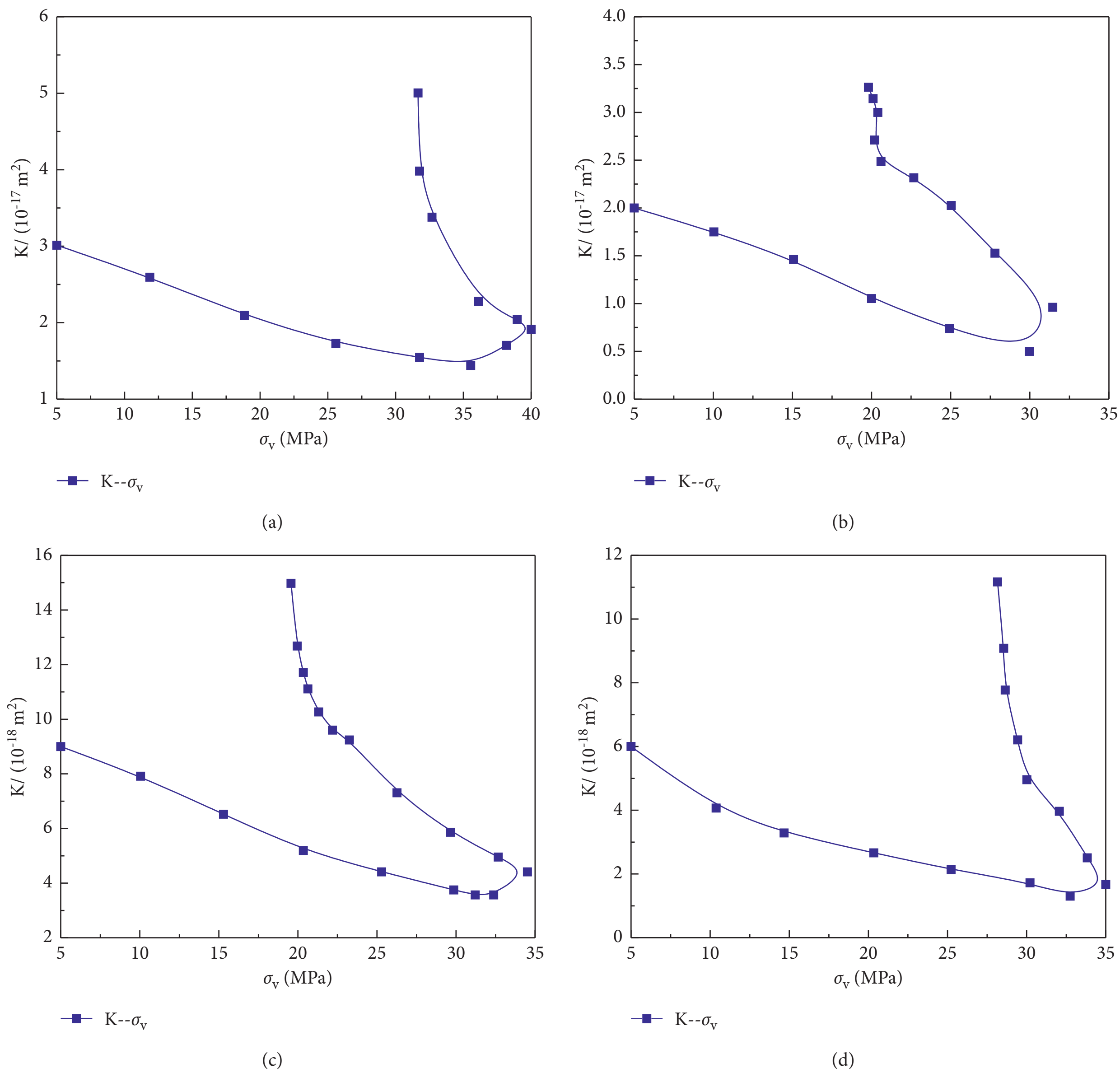

Figure 8: The volumetric stress-percolation rate profile of coal specimens under the condition of different gas pressure at $T = 30°C$. (a) $p = 0.3$ MPa. (b) $p = 0.6$ MPa. (c) $p = 0.9$ MPa. (d) $p = 1.2$ MPa.

Figure 9; that is, (1) the stage when the coal body volume is under compression: With the continuous increase of the main stress, the original fracture pores are gradually compacted, and the volume of the coal body is reduced due to compression, resulting in the squeezing of the seepage channels and the increase of the difficulty for gas permeation. Consequently, the percolation rate is decreased and the volume strain shows the trend of increasing. (2) The stage of coal volume expanding inward: As the main stress continues to increase, the lateral strain slowly begins to exceed axial strain, and the coal gradually starts to expand and develop inward, thus prompting the inward expansion and deformation of coal body volume. In the meantime, more fissures and pores are created inside, making it easier for gas to permeate. The seepage channels are smoother, resulting in higher percolation rate, while the volume strain tends to decrease at this time. The experimental research shows that the percolation rate and volume strain change in inverse proportion at the stage of coal body volume compression deformation and the stage for the inward expansion of coal body volume.

4. Numerical Simulation Analysis

In order to further study the permeability characteristics of gas-containing coal, based on the coal sample prototype of Donghai Coal Mine and the theoretical model of coal rock permeability established by scholars [26, 27], the solid-thermal-gas coupling numerical model of gas-containing coal is constructed by using the solid mechanics, Darcy's law, and the heat transfer interface of porous media in the finite element software COMSOL. The transient solution method

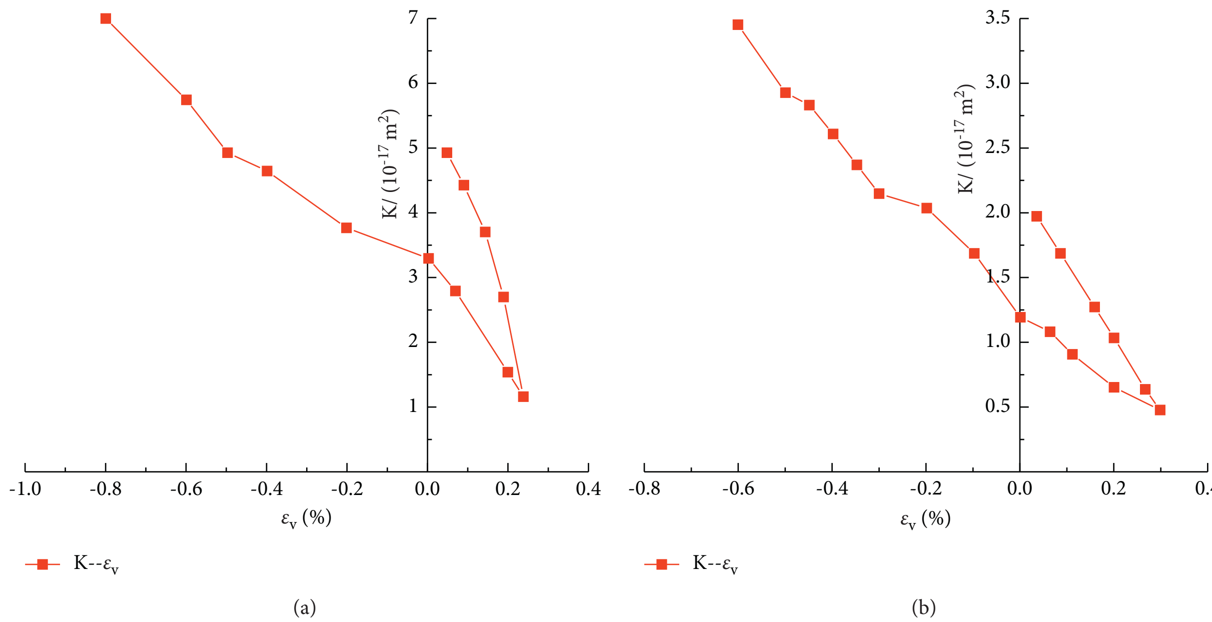

FIGURE 9: The volumetric strain-percolation rate curves of coal specimens under $p = 0.3$ MPa and 0.6 MPa at $T = 30^{\circ}$C. (a) $p = 0.3$ MPa. (b) $p = 0.6$ MPa.

is used to solve the permeability variation and seepage field distribution under the combined action of temperature, main stress, and gas pressure.

The model size is consistent with the experimental coal sample of 50 mm × 50 mm × 100 mm. The initial gas pressure condition was set to 0.1 MPa, which has self-weight effect. The main stress σ_1 and gas pressure are set at the top of the model, and principal stresses σ_2 and σ_3 are set at the left and right end faces and at the front and rear end faces, respectively; that is, boundary load is added at the corresponding end faces of the model. Add displacement constraints at the bottom of the model. The model force diagram is shown in Figure 10, and the model parameters are shown in Table 2.

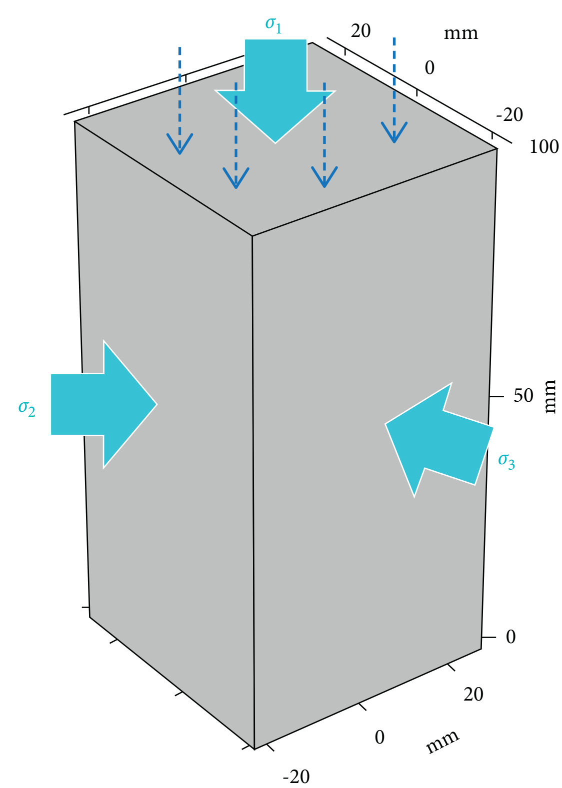

FIGURE 10: Stress diagram of the model.

Figure 11 shows the change of permeability under different gas stress conditions when the temperature is 30°C and the three principal stresses are $\sigma_1 = 3$ MPa, $\sigma_2 = 2$ MPa, and $\sigma_3 = 4$ MPa. It can be seen from the figure that when the temperature and main stress maintain unchanged, the percolation rate decreases with the increase of effective stresses. When the gas pressure increases to 0.6 MPa, the permeability decreases about 56.8% compared with 0.3 MPa. When the gas pressure increases to 0.9 MPa, the permeability decreases about 32.6% compared with 0.6 MPa. When the gas pressure increased to 1.2 MPa, the permeability decreased by about 28.3% compared with 0.9 MPa. When the gas pressure increases to 1.5 MPa, the permeability decreases about 4.7% compared with 1.2 MPa. It can be seen that, with the increase of effective stresses, the decrease rate of permeability gradually tends to be stable from fast to slow. This is because the internal pores of coal in the initial state are developed, but with the increase of gas pressure, the effect on pores is more significant; not only does the internal expansion effect affect the gas seepage channel, but also the Klinkenberg effect is more obvious, so that the permeability

Table 2: Material parameters of numerical model.

Model parameter name	Numerical value
Coal density (kg/m^3)	1450
Elastic modulus (MPa)	2700
Thermal conductivity (J/(m · s · K))	0.443
Specific heat capacity (J/(kg·K))	4.35
Initial permeability (m^2)	$7.6 * 10^{-17}$
Poisson's ratio	0.26
Initial porosity	0.0952
Cubical thermal expansion coefficient	$1.2 * 10^{-4}$ 1/K
Gas density (kg/m^3)	0.714
Initial gas pressure (MPa)	0.1
Gas specific heat rate	1.4
Gas fluid compression ratio	$4 * 10^{-10}$ 1/Pa

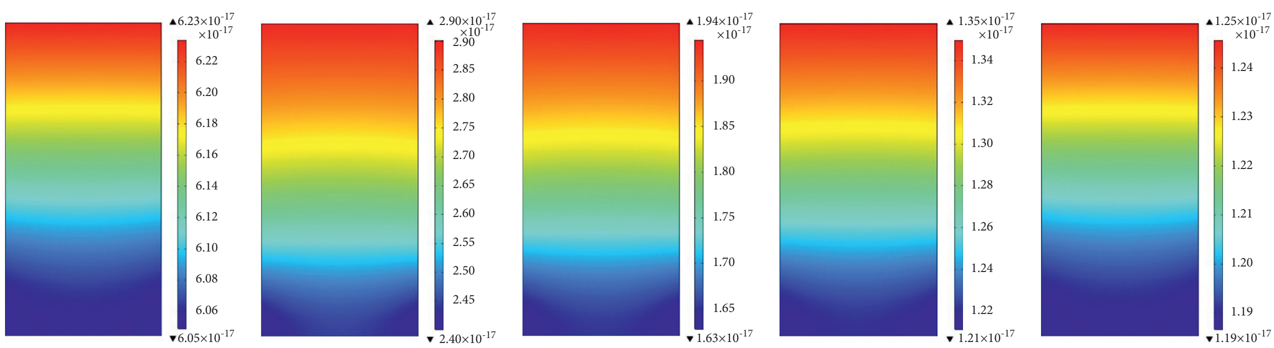

(a) (b) (c) (d) (e)

Figure 11: Permeability distribution under constant temperature and principal stress. (a) $p = 0.3$ MPa. (b) $p = 0.6$ MPa. (c) $p = 0.9$ MPa. (d) $p = 1.2$ MPa. (e) $p = 1.5$ MPa.

of coal shows a trend of rapid decline first and then flattening.

5. Conclusion

(1) Gas pressure, main stress, and temperature have important effects on the percolation rate of gas-filled coal bodies. When temperature and principal stress maintain unchanged, the percolation rate decreases sharply with the increase of gas pressure and then levels off gradually; if the pressure and the main stress maintain unchanged, the percolation rate reduces accordingly when the temperature gradually increases to 70°C; in the process of increasing principal stress, the percolation rate first decreases and then increases, presenting an overall shape of "V." When the main stress increases from 2 MPa to 8 MPa, the original fracture pores are gradually compacted, and the overgrowth of main stress in a certain range will lead to decrease of percolation rate. When the main stress continues to increase, the cracks and pores inside the coal start to expand and develop; therefore, the percolation rate increases.

(2) The internal structure change of coal body and percolation rate are closely related. In the compressive and elastic stages, the overgrowth of strain in a certain range will lead to decrease of percolation rate; when the principal stress increases to the level available to make the coal body enter the yield deformation stage and the damage stage, the changes between the percolation rate and the strain present a direct proportional trend; the percolation rate increases slowly with the increase of strain in the residual stress stage.

(3) In the volumetric compression stage, when the volumetric stress starts to increase, the percolation rate decreases accordingly; as the volumetric stress maintains growth, the coal body cracks and pores start to expand, and there is a sudden increase of percolation rate; in the destruction stage of the coal body, the volumetric stress decreases and the percolation rate increases sharply due to the destruction of its own original load-bearing structure; besides, the load-bearing capacity decreases, and macrocracks appear. There are two main characteristic stages for volumetric strain and gas-filled coal body percolation rate: in the stage when the coal body volume is under pressure, the overgrowth of volumetric stress in a certain range will lead to decrease of percolation rate, while in the stage of coal body volume expanding inward, the percolation rate increases with the decrease of volumetric strain.

Data Availability

The data used to support the findings of this study are available from the corresponding author upon request.

Conflicts of Interest

The authors declare that there are no conflicts of interest regarding the publication of this paper.

Acknowledgments

The research was supported by the Natural Science Foundation of Heilongjiang (ZD2021E006).

References

[1] F. Xiao, L. Duan, and Z. Ge, "Laws of floor breaking in coal mining face and gas extraction application," *Journal of China Coal Society*, vol. 35, no. 3, pp. 417–419, 2010.

[2] X. Zhao, *Study on Gas Migration Law and Prevention Technology of Narrow Coal Pillar Working Face in Inclined Coal seam*, Xi'an University of Science and Technology, Xian, China, 2020.

[3] Y. Yu, H. Zhang, and C. Zhang, "Effects of temperature and stress on the permeability of standard coal briquette specimen," *Journal of China Coal Society*, vol. 38, no. 6, pp. 936–941, 2013.

[4] B. Li, B. Wang, Y. Kang, J. Li, C. Ren, and X. Jiang, "Penetration mechanism of coal rock under combined action of stress and temperature," *Journal of China University of Mining and Technology*, vol. 49, no. 5, pp. 844–855, 2020.

[5] X. Jiang, D. Zhang, S. Peng, W. Nie, L. Wang, and Y. Chen, "Experimental research on impact of temperature on seepage characteristic of coal containing methane under triaxial stress," *Chinese Journal of Rock Mechanics and Engineering*, vol. 30, no. 9, pp. 1848–1853, 2011.

[6] Y. Pan, Y. Zhao, S. Guo, L. Zhao, and H. Wang, "Experimental study on evolution law of mechanical seepage characteristics of coal rock under temperature," *Chinese Mining*, vol. 30, no. 2, pp. 209–213, 2021.

[7] G. Yin, C. Jiang, J. Xu, S. Peng, and W. Li, "Experimental study on thermo-fluid-solid coupling seepage of gas-bearing coal," *Journal of Coal Science and Engineering*, vol. 36, pp. 1495–1500, 2011.

[8] J. Wang, L. Hu, C. Ye, Y. Tang, and P. Yang, "Experimental study on triaxial permeability of marble under complex stress path," *Rockmass Mechanics*, vol. 31, no. 38, pp. 2389–2394, 2010.

[9] Y. Xue, D. Zhang, Y. Yang, and C. Ye, "Permeability analysis of raw coal containing gas under three stresses," *Mining Safety and Environmental Protection*, vol. 47, no. 3, pp. 22–26+31, 2020.

[10] Q. Cheng, "Research on permeability improvement and methane driven effect of hydraulic fracturing for low permeability coal seam," China University of Mining and Technology (Xuzhou), Xuzhou, China, 2012.

[11] F. Xiao, W. Xu, R. Li et al., "Influence of effective pressure on percolation rate of coal," *Advances in Materials Science and Engineering*, vol. 2021, Article ID 5518046, 10 pages, 2021.

[12] X. Yang and Y. Zhang, "Experimental study on the influence of temperature on coal gas permeability under gas-solid coupling," *Journal of Geomechanics*, vol. 14, no. 4, pp. 374–379, 2008.

[13] J. Cao, X. Zhao, and Y. Liu, "Numerical simulation of multiphysical field distribution characteristics of coal and gas outburst," *Mining Safety and Environmental Protection*, vol. 48, no. 2, pp. 7–11, 2021.

[14] R. Lv, S. Peng, and Y. Xu, "Experiment on the relationship between permeability of gas-bearing coal and coal structure," *Journal of Chongqing University*, vol. 35, no. 7, pp. 114–118, 2012.

[15] P. D. Sun, "Numerical simulations for coupled rock deformation and gas leak flow in parallel coal seams," *Geotechnical & Geological Engineering*, vol. 22, pp. 1–17, 2004.

[16] H. Chai, "Analysis on the influence of gas-containing coal permeability," *Shanxi Coking Coal Technology*, vol. 45, no. 1, pp. 43–46, 2021.

[17] S. Valliappan and W. H. Zhang, "Numerical modelling of methane gas migration in dry coal seams," *International Journal for Numerical and Analytical Methods in Geomechanics*, vol. 20, pp. 571–593, 1996.

[18] J. R. Enever and A. Henning, "The relationship between permeability and effective stress for Australian coal and its implications with report to coaled methane exploration and reservoir modeling," in *Proceedings of the 1997 International Coaled Methane Symposium*, pp. 13–22, Tuscaloosa, AL, USA, May 1997.

[19] C. R. Mckee, A. C. Bumb, and A. Koenigr, "Stress dependent permeability and porosity of coal and other geologic formations," *Journal of Central South University*, vol. 3, no. 1, pp. 81–91, 1988.

[20] D. Yonghao, C. Weizhong, W. Guojun, and X. Zhou, "Study on elastoplastic damage model of unsaturated rock mass and its application," *Chinese Journal of Rock Mechanics and Engineering*, vol. 27, no. 4, pp. 728–735, 2008.

[21] X. Zhang, "Experimental and simulation study on instability failure and seepage characteristics of gas-containing coal," *Mining Research and Development*, vol. 40, no. 10, pp. 102–107, 2020.

[22] S. Wu and W. Zhao, "Effective stress analysis of adsorbed CBM-bearing coal," *Chinese Journal of Rock Mechanics and Engineering*, vol. 24, no. 10, pp. 1674–1678, 2005.

[23] S. Zhou and B. Lin, *The Theory of Gas Flow and Storage in Coal Seams*, China Coal Industry Publishing House, Beijing, China, 1990.

[24] C. Liu, G. Zhao, W. Xu et al., "Experimental investigation on failure process and spatio-temporal evolution of rockburst in granite with a prefabricated circular hole," *Journal of Central. South University*, vol. 27, pp. 2930–2944, 2020.

[25] W. Mu, D. Wang, L. Li et al., "Cement flow in interaction rock fractures and its corresponding new construction process in slope engineering," *Construction and Building Materials*, vol. 303, no. 11, Article ID 124533, 2021.

[26] X. Bai, D. Wang, F. Tian, D. Zhang, H. Li, and F. Ren, "Study on permeability model of damaged coal rock under triaxial stress loading and unloading," *Chinese Journal of Rock Mechanics and Engineering*, vol. 40, no. 8, pp. 1536–1546, 2021.

[27] Q. Zeng and Z. Wang, "Stress and temperature sensitivity characteristics of coal rock permeability in eastern Ordos Basin," *Petroleum Science Report*, vol. 5, no. 4, pp. 512–519, 2020.